HTML ABSTRACT + LINKS

Pure-edge dislocation network for strain-relaxed SiGe/Si(001) systems

Akira Sakai,[a] Noriyuki Taoka, Osamu Nakatsuka, and Shigeaki Zaima
Department of Crystalline Materials Science, Graduate School of Engineering, Nagoya University, Furo-cho, Chikusa-ku, Nagoya 464-8603, Japan

Yukio Yasuda
Research Institute of KUT, Kochi University of Technology, Miyanokuchi 185, Tosayamada-cho, Kami-gun, Kochi 782-8502, Japan

(Received 4 January 2005; accepted 27 April 2005; published online 26 May 2005)

We have grown strain-relaxed SiGe layers on Si(001) substrates with a pure-edge dislocation network buried at the heterointerface and analyzed dislocation morphology depending on growth conditions. The process employed here consists of pure-Ge film growth on Si(001) and subsequent high temperature annealing for solid-phase intermixing of the Ge film and Si deposited on the top to form a SiGe alloy layer. Transmission electron microscopy revealed morphological changes of shorter pure-edge dislocation segments initially formed at the Ge/Si interface into a network structure consisting of longer and regularly spaced dislocations during post-deposition annealing. The dislocation network was explicitly preserved even after the intermixing of Si and Ge and predominantly contributed to in-plane strain relaxation of the SiGe layer. Applicability of the pure-edge dislocation network to strain-relaxed SiGe buffer layers on Si(001) substrates is discussed. © *2005 American Institute of Physics*. [DOI: 10.1063/1.1943493]

Strain and defect engineering of SiGe alloy layers is crucial for fabricating high performance metal-oxide-semiconductor field-effect-transistor (MOSFET) devices. Strained Si channel MOSFETs, which specifically require a virtual substrate with an in-plane lattice constant in the range of the lattice constant of Si to that of Ge, have recently gained importance. In general, the introduction of strain into the device requires a highly controlled structure and morphology of dislocations. This is because, in lattice-mismatched materials systems such as SiGe on Si, misfit dislocations play an essential role in relaxing and/or inducing strain and determining structural and electrical properties of crystals which form the device structure. Since dislocations and inhomogeneous strain relevant to the dislocation often induce harmful effects on the carrier mobility of devices,[1,2] a strict control of generation, propagation, and distribution of dislocations is essential.

In diamond lattice structures such as Ge, SiGe, and Si, 60° dislocations are predominantly introduced to relax strain caused by lattice mismatch between a film and a substrate.[3] This is due to the ⟨110⟩/{111} slip system and relatively large Peierls potential. Although several sophisticated growth methods have thus far been employed to introduce 60° dislocations into SiGe/Si(001) systems,[4–7] strain-relaxed SiGe films often exhibit severe surface-roughness, referred to as the cross-hatch pattern, and crystallographic tilting of microscopic domains in the film, i.e., mosaicity. These phenomena are dependent on the structure and distribution of the 60° dislocations: Burgers vectors for these phenomena are tilted with respect to the heterointerface so that dislocation-by-dislocation tilting of SiGe(004) lattice planes inevitably occurs.[8,9] Therefore, the existence of 60° dislocations degrades the crystalline quality of strain-relaxed SiGe to some extent. In order to overcome this problem, it is essential to introduce pure-edge dislocations, the Burgers vectors of which lie not on the {111} but on the (001) plane, parallel to the heterointerface. In this letter, we describe a method to introduce pure-edge dislocations forming a network structure at the SiGe/Si(001) interface by using specific defects initially formed at a pure-Ge/Si(001) interface that was used as a template. Evolution of a pure-edge dislocation network and its impact on the strain relaxation of SiGe layers is examined.

Film growth was achieved using an ultrahigh vacuum solid-source molecular beam epitaxy chamber with a base pressure of less than 1×10^{-10} Torr. The procedure primarily consists of layer-by-layer Ge growth on a clean Si(001) substrate surface, post-deposition annealing (PDA) in ultrahigh vacuum for strain relaxation of the Ge film, and high temperature annealing (HTA) in a N_2 ambient for 2 min for solid-phase intermixing of the Ge film and a Si layer deposited on the top. The layer-by-layer Ge growth was carried out with an alternative method of low-temperature growth at 200 °C or hydrogen-surfactant epitaxy. Details of the hydrogen-surfactant epitaxy have been published earlier.[10,11] No significant differences in the final structures of Ge and SiGe films were observed between these two growth methods. Transmission electron microscopy (TEM), x-ray diffraction (XRD), and secondary ion mass spectrometry (SIMS) were used to characterize dislocation structures, crystallinity and the lattice constant, and concentration of Ge, respectively.

First, we examine PDA-induced morphological changes of dislocations in Ge films on Si. Figure 1 shows plan-view TEM images of 20-nm-thick Ge/Si(001) samples grown by hydrogen-surfactant epitaxy at 300 °C. The samples were subjected to PDA at various temperatures. As can be clearly seen in Fig. 1(a), the as-grown sample contains short segments of dislocations that lie preferentially along the [110] direction perpendicular to the reflection vector $\mathbf{g}=[2\bar{2}0]$. An image of the same area with an orthogonal $\mathbf{g}$ revealed that these segments were out of contrast and instead similar dislocation morphology appeared along the $[1\bar{1}0]$ direction. Thus these segments are found to possess a pure-edge char-

[a]Electronic mail: sakai@alice.xtal.nagoya-u.ac.jp

Downloaded 18 Oct 2006 to 133.6.32.11. Redistribution subject to AIP license or copyright, see http://apl.aip.org/apl/copyright.jsp

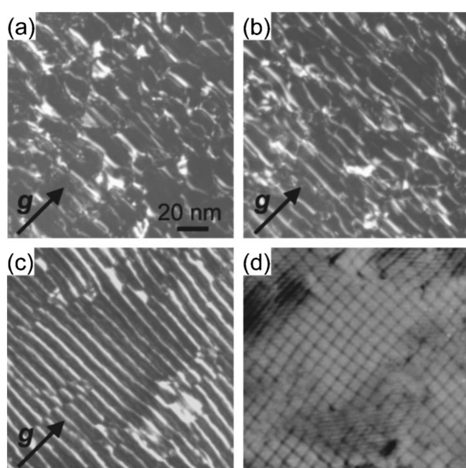

FIG. 1. Plan-view dark-field TEM images of (a) as-grown, (b) 430 °C annealed, and (c) 680 °C annealed 20-nm-thick Ge/Si(001) samples. Annealing duration was 10 min. These images were taken by the weak-beam method under the condition of **g**/3**g** with **g**=[$2\bar{2}0$]; (d) plan-view bright-field TEM image taken from the same area as (c), showing the network morphology of pure-edge dislocations. The image was taken under the condition that the incident electron beam is slightly tilted to the [400] direction from the on-axis [001] direction.

acter, their Burgers vector explicitly lies on the (001) plane, and they align along two orthogonal ⟨110⟩ directions. The formation of this type of pure-edge dislocation segments has also been confirmed for low-temperature-grown Ge films on Si(001).[12] It should be noted that the segments elongate along their line direction and become straight after PDA, as shown in Figs. 1(b) and 1(c). Longer and more regularly spaced pure-edge dislocations are formed at a higher temperature of PDA. As a result, as shown in Fig. 1(d), a network morphology consisting of pure-edge dislocations lined up regularly with a spacing of ~10 nm can be realized at the Ge/Si(001) interface.

Characters of defects existing in the Ge/Si(001) samples at each PDA stage were analyzed by employing cross-sectional high-resolution TEM observation. Table I summarizes the percentage of defects in the samples as a function of PDA conditions. Stacking faults progressively decreased and disappeared with an increase in PDA temperature. Defects with a Burgers vector lying on (001), including pure-edge dislocations, were observed only at the interface at any given stage and these became dominant after 680 °C PDA. On the other hand, threading defects with Burgers vectors on {111}

TABLE I. Percentage of defects in the samples observed in the range over 10 μm as a function of PDA conditions. Defect characters were determined by cross-sectional high-resolution TEM.

Sample	As-grown	After 430 °C PDA	After 680 °C PDA
Threading defect with Burgers vector on (001)	0	0	0
Interfacial defect with Burgers vector on (001)	39	48	87
Threading defect with Burgers vector on {111}	10	27	2
Interfacial defect with Burgers vector on {111}	22	15	11
Stacking fault	29	10	0
			(%)

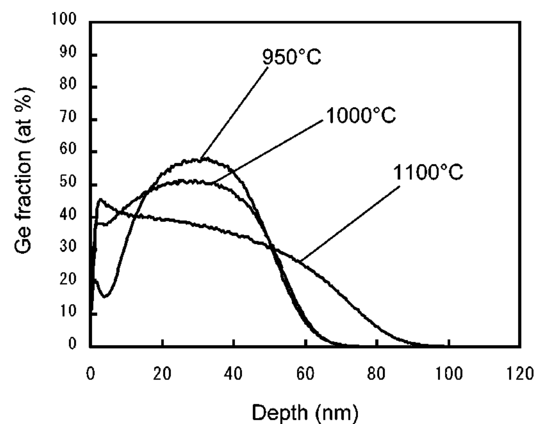

FIG. 2. SIMS depth profiles of Ge in Si (17 nm)/Ge (35 nm)/Si(001) samples after HTA at 950, 1000, and 1100 °C for 2 min in a N_2 ambient.

increased after 430 °C PDA but drastically decreased after 680 °C PDA. This result and the above plan-view TEM images in Fig. 1 strongly suggest that the propagation of pure-edge segments forming long straight dislocations is mainly promoted by the glide motion of threading arms, such as 60° dislocations, accompanying the interfacial pure-edge segment. The regular lineup of dislocations is probably realized with a climb motion of the pure-edge segments during PDA although the possibility that slip systems other than ⟨110⟩/{111} may operate at higher stresses than the present case.[13]

Employing this pure-edge dislocation network as a template, a control over dislocation morphology for growing SiGe layers was achieved. Figure 2 shows SIMS depth profiles of Ge for Si (17 nm)/Ge (35 nm)/Si(001) samples after HTA, at various temperatures. Interdiffusion, both at the deposited-Si/Ge and Ge/substrate-Si interfaces, is clearly observed: the former is promoted at a lower temperature than the latter. Consequently, the solid-phase intermixing of Si and Ge leads to the formation of SiGe alloy layers. Corresponding plan-view TEM images of dislocation morphology in the HTA samples are shown in Figs. 3(a)–3(c). It should be noted that a pure-edge dislocation network similar to the one initially formed at the Ge/Si(001) interface, as shown in

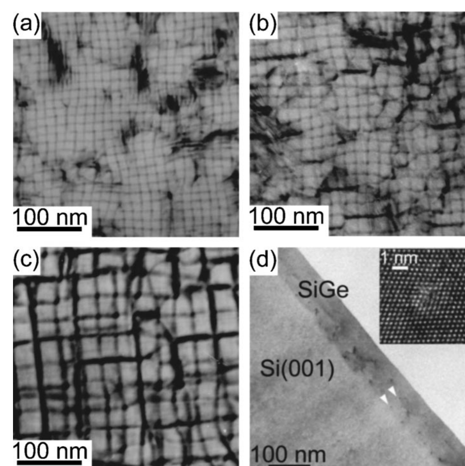

FIG. 3. Plan-view TEM images of Si (17 nm)/Ge (35 nm)/Si(001) samples after HTA at (a) 950 °C; (b) 1000 °C; and (c) 1100 °C. These images were taken under the same condition as that shown in Fig. 1(d); (d) cross-sectional TEM image of the sample shown in (c). Inset shows a closeup high-resolution TEM image of an end-on dislocation indicated by a lower arrow head.

Downloaded 18 Oct 2006 to 133.6.32.11. Redistribution subject to AIP license or copyright, see http://apl.aip.org/apl/copyright.jsp

Fig. 1(d), was still observed even after forming a SiGe alloy layer due to HTA. Furthermore, wider spacing of individual pure-edge dislocations are clearly observed at higher temperatures. A cross-sectional view of the sample annealed at 1100 °C is shown in Fig. 3(d). End-on dislocations located periodically were found to have an explicit pure-edge character, as seen in the inset.

Taking the SIMS and TEM results into account, dislocation behaviors during HTA can be deduced. The solid-phase intermixing of Si and Ge caused by HTA results in the formation of a SiGe alloy layer. Since the initial Ge film is fully strain-relaxed with a pure-edge dislocation network buried at the interface, it is concomitantly subjected to tensile stress with the change into a SiGe phase. Possibly, this stress produces forces exerted on the pure-edge dislocation and thus some of the dislocations can climb to the surface of the film, resulting in the reduced density at the interface. Formation of a stacked structure of pure-edge dislocations, as indicated by arrow heads in Fig. 3(d), strongly suggests the occurrence of interaction among the climbing dislocations during HTA, resulting in an energetically favorable morphology.[3]

In-plane lattice spacings of SiGe layers were also measured in the same samples as those shown in Fig. 3, and are considered to be a function of HTA temperature. Figure 4 shows three sets of data for the {110} lattice spacings; those directly measured by XRD two-dimensional reciprocal space mapping,[14,15] those derived from the spacing of pure-edge dislocations observed in the plan-view TEM images shown in Fig. 3, and those calculated by assuming nonstrained SiGe crystals with average Ge concentrations obtained from SIMS data shown in Fig. 2. The {110} lattice spacing decreases monotonically with the increase in the annealing temperature, possibly due to Si in-diffusion to the Ge layer. Observed correspondence between two sets of data from XRD and TEM implies that the pure-edge dislocation network predominantly contributes to the in-plane strain relaxation of SiGe. On the other hand, a comparison between the measured {110} lattice spacings and the calculated values based on the SIMS result clearly indicates that the SiGe layer obtained here contains in-plane biaxial tensile strain. This implies that excess dislocation persists in the film even after HTA.

Finally, on the basis of the principle feature that the pure-edge dislocation has a Burgers vector lying on the (001) plane, the applicability of the pure-edge dislocation network to the strain relaxation of SiGe buffer layers on Si(001) substrates is discussed. First, no tilting and no rotation of microscopic domains are expected in the strain-relaxed SiGe layer. This leads to strict suppression of mosaicity, and this has recently been verified by using XRD two-dimensional reciprocal space mapping.[14] Second, contrary to the 60° dislocation, one pure-edge dislocation line on (001) induces line symmetry of strain distribution on the (001) plane. Since the cross-hatch pattern is known to be closely related to asymmetric strain distribution caused by the 60° dislocation,[7,16] this feature might effectively suppress the surface roughening during growth. Third, the pure-edge dislocation is sessile and thus more thermally stable than glissile dislocations. Fourth, since the Burgers vector of the pure-edge dislocation is twice as effective in relaxing the in-plane ⟨110⟩ strain as compared to that of the 60° dislocation, only half the number density is enough to relax the same amount of strain. The present study only offers preliminary results for approaching device-grade crystalline quality of SiGe buffer layers used for practical strained Si channel MOSFETs. Nevertheless, the above considerations give rise to the fascinating concept of the superiority of the method of applying the pure-edge dislocation network to the SiGe/Si systems.

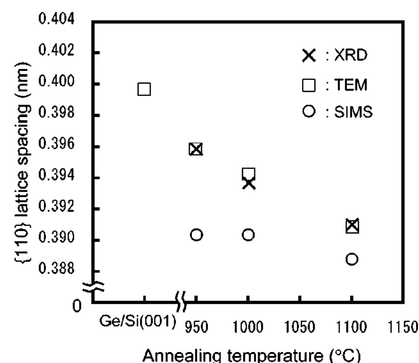

FIG. 4. {110} lattice spacings of SiGe layers as a function of HTA temperature. Three sets of data are shown; the {110} lattice spacings measured by XRD two-dimensional reciprocal space mapping, those derived from the spacings of pure-edge dislocations observed in the plan-view TEM images shown in Fig. 3, and those calculated for nonstrained SiGe crystals with average Ge concentrations obtained from SIMS data shown in Fig. 2.

To summarize, strain-relaxation of SiGe buffer layers on Si(001) substrates with a pure-edge dislocation network buried at the heterointerface has been demonstrated. Dislocation behaviors forming a network morphology at the pregrown Ge/Si(001) interface were revealed by TEM. The pure-edge dislocation network initially formed at the Ge/Si(001) interface was retained even after the intermixing of Si and Ge and predominantly contributed to the in-plane strain relaxation of SiGe layers. The present method introduces fundamental changes in the manner of strain relaxation of SiGe on Si(001) and raises the possibility of solving problems caused by the conventional 60° dislocation.

[1] K. Ismail, F. K. LeGoues, K. L. Saenger, M. Arafa, J. O. Chu, P. M. Mooney, and B. S. Meyerson, Phys. Rev. Lett. **73**, 3447 (1994).
[2] N. Sugii, K. Nakagawa, S. Yamaguchi, and M. Miyao, Appl. Phys. Lett. **75**, 2948 (1999).
[3] J. P. Hirth and J. Lothe, *Theory of Dislocations* (Krieger, Malabar, FL, 1992).
[4] B. S. Meyerson, J. F. Morar, and F. K. LeGoues, Appl. Phys. Lett. **53**, 2555 (1988).
[5] A. Sakai, K. Sugimoto, T. Yamamoto, M. Okada, H. Ikeda, Y. Yasuda, and S. Zaima, Appl. Phys. Lett. **79**, 3398 (2001).
[6] A. D. Capewell, T. J. Grasby, T. E. Whall, and E. H. C. Parker, Appl. Phys. Lett. **81**, 4775 (2002).
[7] E. A. Fitzgerald and S. B. Samavedam, Thin Solid Films **294**, 3 (1997).
[8] P. Y. Timbrell, J.-M. Baribeau, D. J. Lockwood, and J. P. McCaffrey, J. Appl. Phys. **67**, 6292 (1990).
[9] P. M. Mooney, F. K. LeGoues, J. O. Chu, and S. F. Nelson, Appl. Phys. Lett. **62**, 3464 (1993).
[10] A. Sakai and T. Tatsumi, Appl. Phys. Lett. **64**, 52 (1994).
[11] A. Sakai, T. Tatsumi, and K. Aoyama, Appl. Phys. Lett. **71**, 3510 (1997).
[12] D. J. Eaglesham and M. Cerullo, Appl. Phys. Lett. **58**, 2276 (1991).
[13] M. Albrecht, H. P. Strunk, R. Hull, and J. M. Bonar, Appl. Phys. Lett. **62**, 2206 (1993).
[14] T. Yamamoto, A. Sakai, T. Egawa, N. Taoka, O. Nakatsuka, S. Zaima, and Y. Yasuda, Appl. Surf. Sci. **224**, 108 (2004).
[15] N. Taoka, A. Sakai, T. Egawa, O. Nakatsuka, S. Zaima, and Y. Yasuda, Mater. Sci. Semicond. Process. **8**, 131 (2005).
[16] M. A. Lutz, R. M. Feenstra, F. K. LeGoues, P. M. Mooney, and J. O. Chu, Appl. Phys. Lett. **66**, 724 (1995).

Downloaded 18 Oct 2006 to 133.6.32.11. Redistribution subject to AIP license or copyright, see http://apl.aip.org/apl/copyright.jsp